Supplementary Information: The origin of high thermal conductivity and ultra-low thermal expansion in copper-graphite composites

Izabela Firkowska, André Boden, Benji Boerner, and Stephanie Reich

S1 Thermal diffusivity and specific heat of SuCoLEx

The thermal diffusivity was derived from flash measurements. Both the thermal diffusivity in *x* and *z* direction were measured, using a special sample holder for anisotropic measurements (Fig. 1Sa). The specific heat was derived from the flash measurements by comparing the signal to a reference measurement. The resulting values are in agreement with the predictions made by the rule of mixture (Fig. 1Sb). The thermal conductivity in *x* and *z* direction was calculated by multiplying thermal diffusivity, specific heat, and density (measured by Archimedes' principle).

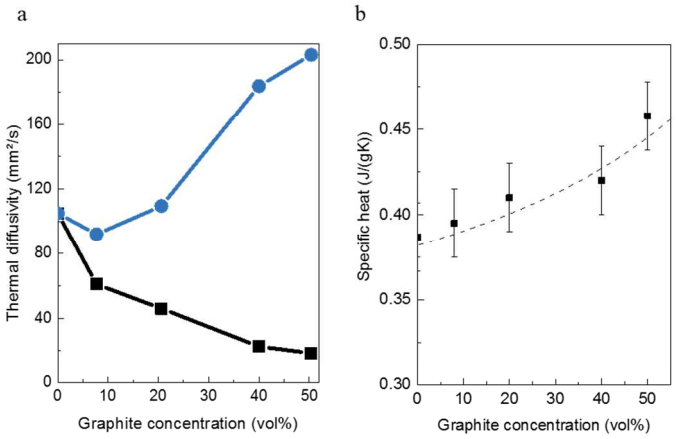

Supplementary Figure 1S a, Thermal diffusivity in α_x (●) and α_z (■) direction and **b,** specific heat of SuCoLEx (■) in dependence of the graphite concentration in comparison to the rule of mixture (dashed line).

S2 SuCoLEx characterization

The crystalline quality of the graphite flakes was accessed by their Raman spectra. The ratio between the D (1320cm^{-1}) and the G peak (1580cm^{-1}) was measured after each preparation step and compared to the as received material (Fig.2S). Ball milling increased the D/G-intensity ratio

from 0.21 to 0.27 indicating a slightly increased disorder introduced to the graphite particles. After spark plasma sintering the ratio was 0.28 showing that the consolidation process did not increase the disorder in graphite.

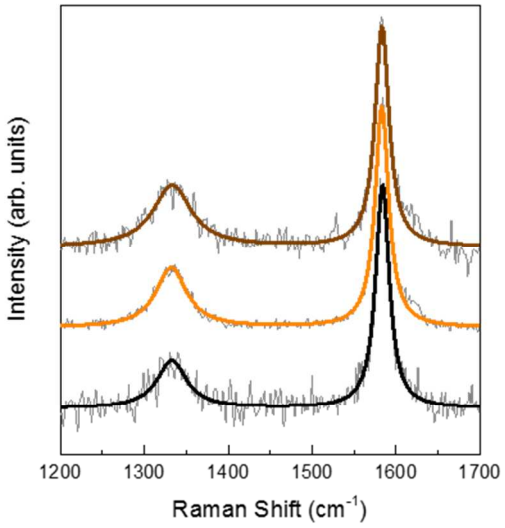

Supplementary Figure 2S Raman spectra of graphite particles as received (bottom), after ball milling (middle) and after SPS (top).

S3 Polarized Raman spectroscopy in graphite and analysis of graphite alignment

In an earlier study we derived the expression for obtaining the graphite platelet alignment from the polarization-angle dependence of the G peak Raman intensity[1] by using the selection rules for light scattering in crystals to obtain the intensity of the Raman active modes for an individual graphite platelet[2] and then integrating over all possible orientation angles. The overall intensity of graphite platelets in a composite material is then given by[1]

$$I_{tot} \propto \iint g(\gamma_1, \sigma_G)\, g(\gamma_2, \sigma_G)\, I_G(\gamma_1, \gamma_2)\; d\gamma_1 d\gamma_2 + I_0. \qquad (1)$$

with

$$g(\gamma, \sigma) = \frac{1}{\sigma\sqrt{2\pi}} \exp\left(-\frac{\gamma^2}{2\sigma^2}\right),$$

where $g(\gamma,\sigma_G)$ is the angle distribution for the rotation angles γ_1 and γ_2 and I_0 is a correction term for the Raman setup. Thus, the standard deviation σ_G remains the only fitting parameter for the

intensity of the graphite platelets within the copper matrix. We obtain σ_G=0.69 for 8vol%, σ_G=0.61 for 20vol% and σ_G=0.37 for graphite content above 20vol%. The graphite alignment was tuned by the concentration.

S4 Thermal conductivity of SuCoLEx within an effective medium approximation

To compare the thermal conductivity of SuCoLEx to modeling predictions we use an effective medium approximation developed by Nan *et al.*.[3,4] This model allows to calculate the thermal conductivity in dependence of the concentration, geometry, the intrinsic thermal conductivity of the composite components and the thermal interface resistance as well as the orientation of the filler. The statistical orientation of the graphite particles is represented by $\langle cos^2\theta \rangle$ which equals 1/3 for totally randomly oriented particles and becomes one for fully aligned fillers. It is given by[4]

$$\langle cos^2\theta \rangle = \frac{\int \varphi(\theta)\, cos^2\theta\, sin\theta\, d\theta}{\int \varphi(\theta)\, sin\theta\, d\theta}, \tag{10}$$

with

$$\varphi(\theta) = \frac{1}{\sigma\sqrt{2\pi}} \exp\left(-\frac{\theta^2}{2\sigma^2}\right)$$

where θ is the angle between the symmetry axes of the composite and the graphite particles and $\varphi(\theta)$ describes the statistical distribution of θ using σ as determined by Raman measurements. For a graphite concentration of 40 and 50 vol% $\langle cos^2\theta \rangle$ was found to be 0.80. However, the degree of alignment is lower for 8 and 20 vol% with a statistical orientation of 0.54 and 0.58, respectively. As shown, using $\langle cos^2\theta \rangle$ = 0.80 to calculate the thermal conductivity leads to very good agreement for graphite concentrations of 40 and 50 vol% (Fig. 2) but not for 8 and 20 vol%. Therefore, the thermal conductivity is calculated for $\langle cos^2\theta \rangle$ of 0.54 and 0.58, respectively, and shown in Fig. 4S. Using the corresponding orientation factors for 8 and 20 vol% leads to good agreement between the calculated thermal conductivity and the measured data.

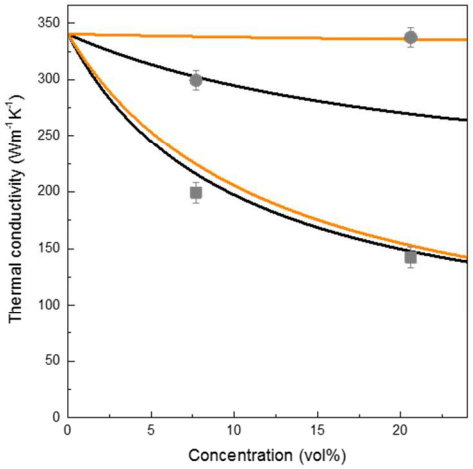

Supplementary Figure 4S Experimental data of k_x (●) and k_z (■) together with the effective medium approximation for the orientation parameter of 8vol% SuCoLEx (black) and 20vol% SuCoLEx (orange).

To point out the importance of the platelet alignment for the superior thermal conductivity k_x is calculated for $\langle cos^2\theta \rangle$ of 1.00 (full alignment), 0.80 and 0.50 (Fig5Sa). Fully aligned platelets show by far the highest conductivity values whereas poorly aligned platelets lead to thermal conductivity below the value of the matrix material. This correlation points out that the alignment is the key factor for a high thermal conductivity in SuCoLEx. On the other hand the thermal interface resistance between copper and the graphite platelets is not a major limiting factor for the thermal conductivity. The calculation with ten times higher Kapitza resistance results in a small decrease of the thermal conductivity k_x (Fig5Sb). Even with 100 times higher Kapitza resistance the resulting k_x is higher than the matrix conductivity.

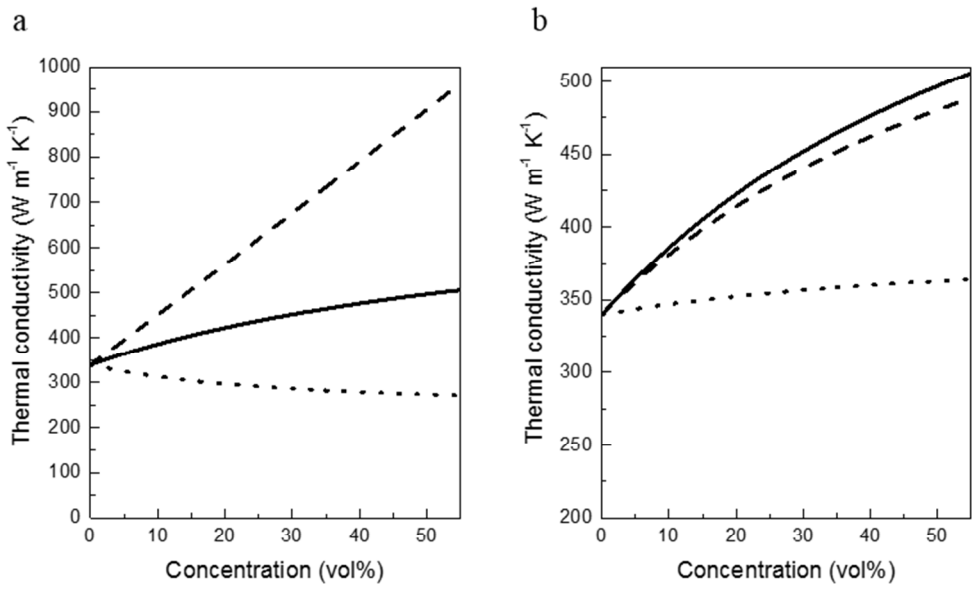

Supplementary Figure 5S a, thermal conductivity k_x for different platelet alignments $\langle cos^2\theta \rangle$ of 1.00 (dashed), 0.80 (solid), and 0.50 (dotted). **b,** thermal conductivity k_x for different Kapitza resistances of 10^{-9}m^{2}KW^{-1} (solid), 10^{-8}m^{2}KW^{-1} (dashed), and 10^{-7}m^{2}KW^{-1} (dotted).

S5 Thermal stress/strain measurements with micro-Raman spectrometer

A strain in a crystal leads to a shift and splitting of the phonon frequencies. The effect of a general strain tensor on the Raman modes of Si is described by the secular equation[5]

$$\begin{vmatrix} p\varepsilon_{11}+q(\varepsilon_{22}+\varepsilon_{33})-\lambda & 2r\varepsilon_{12} & 2r\varepsilon_{13} \\ 2r\varepsilon_{12} & p\varepsilon_{22}+q(\varepsilon_{11}+\varepsilon_{33})-\lambda & 2r\varepsilon_{23} \\ 2r\varepsilon_{13} & 2r\varepsilon_{23} & p\varepsilon_{33}+q(\varepsilon_{11}+\varepsilon_{22})-\lambda \end{vmatrix} = 0. \qquad (11)$$

p, q, and r are material parameters representing the phonon deformation potential. Unstrained silicon has a triply-degenerate optical phonon ($\omega_0 = 522$ cm^{-1}) for zero wavevector. The degeneracy is lifted with strain. The eigenvalues of the secular equation predict the Raman frequency shifts with strain $\Delta\omega_i = \omega_i - \omega_0 = \lambda_i/2\omega_0$. The intensity of the Raman signal for each optical mode ω_i depends on the polarization direction of the incident and scattered light and the strain tensor $\boldsymbol{\varepsilon}$. Our setup limited the observation to the LO mode along the SuCoLEx z direction. It corresponds to the third eigenvalue of Eq.(11), $\Delta\omega_3 = [p\varepsilon_{33} + q(\varepsilon_{11} + \varepsilon_{22})]/2\omega_0$.

S6 Cooling performance of SuCoLEx for high-power LEDs

To test the heat dissipation performance of SuCoLEx the high-power LEDs (3W, white, WTN-3W-190kw) were mounted on a copper and SuCoLEx (20wt% Gr) with a thermally conductive silver-based adhesive (Pyro-Duct 597-A). The samples were additionally attached to the aluminum block. The heat flux and diode temperature were monitored with an infrared camera.

To ensure that both diodes are similar in terms of performance, they were selectively measured and selected from a group of several identical diodes. The connection of two diodes was parallel with an LED power supply. In order to provide reliable thermal image interpretation, the adhesive emission tape, with defined emission factor 0.95 was attached to the samples surface at the measuring point. Otherwise, the untreated surface of the SuCoLEx and copper with different emission factor makes a quantitative evaluation impossible.

References

1. Boden, A., Boerner, B., Kusch, P., Firkowska, I. & Reich, S. Nanoplatelet Size to Control the Alignment and Thermal Conductivity in Copper–Graphite Composites. *Nano Lett.* **14,** 3640–3644 (2014).
2. Cardona, M. in *Light Scattering in Solids II* (eds. Cardona, P. D. M. & Güntherodt, P. D. G.) 19–178 (Springer Berlin Heidelberg, 1982). at <http://link.springer.com/chapter/10.1007/3-540-11380-0_14>
3. Nan, C.-W. Physics of inhomogeneous inorganic materials. *Prog. Mater. Sci.* **37,** 1–116 (1993).
4. Nan, C.-W., Birringer, R., Clarke, D. R. & Gleiter, H. Effective thermal conductivity of particulate composites with interfacial thermal resistance. *J. Appl. Phys.* **81,** 6692 (1997).
5. Cerdeira, F., Buchenauer, C. J., Pollak, F. H. & Cardona, M. Stress-Induced Shifts of First-Order Raman Frequencies of Diamond- and Zinc-Blende-Type Semiconductors. *Phys. Rev. B* **5,** 580–593 (1972).